The Influence of Side-Chain Position on the Optoelectronic Properties of a Red-Emitting Conjugated Polymer

Li Ping Lu,* Chris E. Finlayson, Dinesh Kabra,* Sebastian Albert-Seifried, Myoung Hoon Song, Remco W. A. Havenith, Guoli Tu, Wilhelm T. S. Huck, Richard H. Friend*

A study of the organic semiconductor F8TBT is presented, directly comparing a conventional form (F8TBT-out) with a form with varied alkyl side-chain position (F8TBT-in), in terms of optical properties and device performance in light-emitting-diodes (LEDs). Computational simulations of the side-chain position with respect to the TBT unit reveal geometrical differences between F8TBT-out and F8TBT-in. π–π conjugation on the backbone of F8TBT-in is interrupted by a distortion of the benzothiadiazole ring, leading to a blue-shift of the absorption spectrum and increased photoluminescence quantum efficiency. Both conventional and hybrid LEDs demonstrate that devices with F8TBT-in show improved performance, as compared to F8TBT-out, illustrating how tuning the optoelectronic properties of conjugated polymers by varying the placement of side chains has an important role in device optimization.

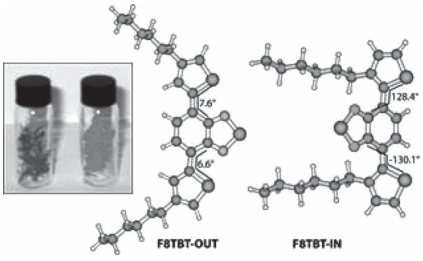

1. Introduction

One of the great advantages of the polyfluorene (PFO) polymer family is that the electrical and optical properties can be tuned through modification of the chemical structure. In the context of semiconducting polymer-based light-emitting diode (LEDs), the emission color of PFOs can be tuned over the entire visible range by introducing

Dr. L. P. Lu, Dr. S. Albert-Seifried, Prof. R. H. Friend
Cavendish Laboratory, University of Cambridge, Cambridge CB3 0HE, UK
E-mail: lpl23@cam.ac.uk; rhf10@cam.ac.uk
Dr. C. E. Finlayson
Institute of Mathematical & Physical Sciences, Prifysgol Aberystwyth University, Wales SY23 3BZ, UK
Dr. D. Kabra
Department of Physics, Indian Institute of Technology Bombay, Powai Mumbai, India
E-mail: dkabra@iitb.ac.in
Dr. M. H. Song
School of Mechanical & Advanced Materials Engineering, Ulsan National Institute of Science & Technology, UNIST-gil 50, Ulsan 689-805, Republic of Korea
Dr. R. W. A. Havenith
Theoretical Chemistry, Zernike Institute for Advanced Materials, University of Groningen, Nijenborgh 4, 9747 AG Groningen, The Netherlands
Dr. G. Tu
Wuhan National Laboratory for Optoelectronics, Huazhong University of Science and Technology, Luoyu Road, Wuhan 430074, China
Prof. W. T. S. Huck
Radboud University Nijmegen, Institute for Molecules and Materials, Heyendaalseweg 135, 6525 AJ Nijmegen, The Netherlands

DOI: 10.1002/macp.201200681

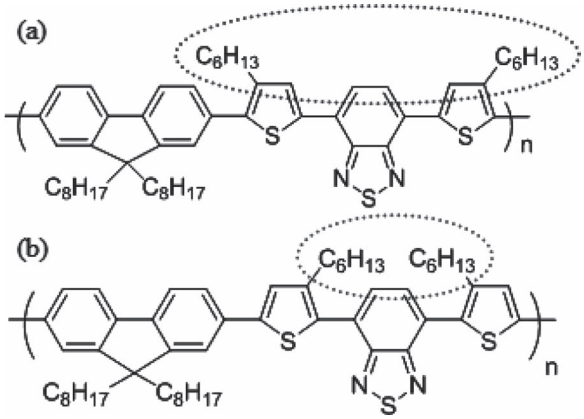

Figure 1. The chemical structures of: a) conventional F8TBT, referred to as "F8TBT-out" in this work, and b) "F8TBT-in", with different side-chain positioning in comparison to (a).

narrow-bandgap comonomers into the PFO backbone,[1] or by variation of the side chains.[2] F8TBT (or poly((9,9-dioctylfluorene)-2.7-diyl-alt-[4,7-bis(3-hexylthien-f-yl)-2,1,3-benzothiadiazole]-2′,2″-diyl)) is a PFO emitting a saturated red color; as the name suggests, it is derived from fluorene F8 and 4,7-bis(3-hexylthien)-2,1,3-benzothiadiazole, TBT units. The structure shown in Figure 1a F8TBT is a typical alternating A-B type copolymer synthesized via Suzuki coupling by the introduction of a low-bandgap monomer, namely the TBT unit. A characteristic of polymers synthesized by Suzuki coupling is that, if the narrow-bandgap component is less than or equal to 50% of the copolymer, each individual narrow-bandgap unit is separated on both sides by wide-bandgap segments.[3] The narrow-bandgap segment can therefore function as an exciton trap, which facilitates efficient intramolecular energy transfer from the fluorene segment to the TBT unit, leading to a saturated red emission if F8TBT is used as an emissive layer in polymer LEDs and optically pumped lasers.[3–5]

While F8TBT was originally developed as a red-emitting polymer for LED applications,[3,6] it has been extensively used as a good candidate for polymer solar cell devices, due to its ambipolar characteristics, whereby it can act as electron donor and hole transporter in blends with PCBM or CdSe nanocrystals,[7–9] as well as electron acceptor and electron transporter in blends with P3HT.[10,11] For photovoltaics applications, the composition of F8TBT has a 1:1 ratio of F8 to TBT, while for electroluminescence (EL) applications TBT concentrations of 15% show the best performance. The ambipolar characteristics of F8TBT, as demonstrated in solar cell and light-emitting field-effect transistors,[12] can also be exploited by hybrid LED architectures, in order to keep the recombination zone (RZ) away from the injecting electrodes.[13] Compared with a highly efficient green light-emitting PFO copolymer, such as F8BT derived from fluorene and benzothiadiazole, the LED device efficiency with red-emitters is typically low and the goal of high-efficiency polymer emitters with saturated red emission remains a great challenge.[14] Cambridge Display Technology (CDT) reported a saturated red emitter with a high external quantum efficiency of 3%, however the chemical structure is not disclosed.[15]A significant improvement was reported by Cao and co-workers[16]; upon variation of the concentration of TBT units, from 1% to 50% with respect to the F8 unit, it was found that the device performance improves with increasing TBT concentration, and reaches a maximal luminance of ≈351 cd m^{-2} when the TBT unit concentration is ≈15%.[3,16] They also introduced alkyl side chains on the thiophene rings to increase the solubility of the polymer. As expected, the PL efficiency of the copolymer with alkyl side chains, namely F8TBT, is significantly enhanced in the solid state in comparison with its unsubstituted analogue, poly[2,7-(9,9-dioctylfluorene)-alt-4,7-bis(thiophen-2-yl)benzo-2,1,3-thiadiazole] (PFO-DBT).[16] Furthermore, the LEDs based on F8TBT show around twice the device efficiency (external quantum efficiency (EQE) and current efficiency), when compared with the unsubstituted equivalent, PFO-DBT. The alkyl substitution on the thiophene rings in F8TBT greatly reduces the interchain interaction by preventing close packing and thereby reduces concentration quenching of F8TBT chains in comparison with its parent analogue, the PFO-DBT copolymer.[3,16–18]

In this paper, a study of the optical and electrical properties with respect to the alkyl side-chain position on the thiophene rings in F8TBT is reported. The conventional F8TBT, called "F8TBT-out", and the F8TBT with varied alkyl side-chain position, called "F8TBT-in", are compared side by side in terms of optical properties and the device performance in conventional- and hybrid light-emitting diode structures. The chemical structures of F8TBT-out and F8TBT–in are shown in Figure 1a and b, respectively. The varied F8TBT-in (Figure 1b) with two alkyl side chains inwards is likely to introduce more steric hindrance and further prevent the close packing of the interchains of the polymer, as compared with the F8TBT-out. A photographic image of the as-synthesized copolymers F8TBT-out and F8TBT-in, which evidently exhibit different visual colors, is shown in the Graphical Abstract figure for this paper (F8TBT-out on the left, and F8TBT-in on the right). This is apparently the consequence of side chain position modification, since this can influence the intra- and intermolecular interactions, and thus tune the optical and electrical properties.[2] In this work, the F8TBT-in copolymer is found to have an enhanced photoluminescence quantum efficiency (PLQE) in the solid state, as compared with F8TBT-out. The radiative and non-radiative decay constants are also derived from fluorescence decay lifetime

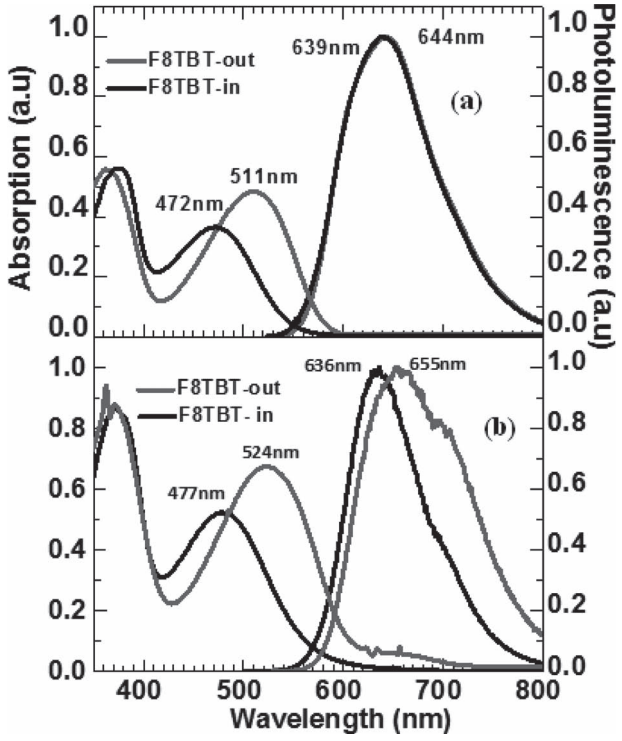

Figure 2. The photoluminescence and absorption spectra of F8TBT-out (gray) and F8TBT-in (black): in p-xylene solution (a); in film (b).

measurements. A computational simulation, focusing on the side-chain position with respect to the TBT units, reveals a different geometry of the backbone chain in these F8TBT-in and F8TBT-out polymers. Studies of device performance in both conventional- and hybrid LEDs demonstrate that the device with F8TBT-in as the emissive layer shows an improved performance, as compared with the device based on the polymer F8TBT-out. We consider how the concept of using molecular design to tune the optical and electrical properties, based on theoretical predictions, may be implemented experimentally.

2. Results

The polymers F8TBT-out and F8TBT-in were synthesized by Huck et al. in the Chemistry Department, University of Cambridge,[17] and the F8TBT-in and F8TBT-out used in this study have a molecular weight ($\overline{M}_w$) of 50k g mol^{-1}. For optical measurements, 100 nm thick films were made by dissolving the polymers in p-xylene and then spin-coating onto quartz substrates.

2.1. Optical Properties of F8TBT-in and F8TBT-out

Figure 2 illustrates the absorption and fluorescence spectra of F8TBT-in and F8TBT-out in both solution and thin film, as a function of wavelength. The absorption spectra resulting from solution and film show two peaks within the visible range, the peak around 470 nm stems from the HOMO–LUMO transition of F8TBT-in and the peak around 500 nm is attributed to that of F8TBT-out. The absorption spectrum of F8TBT-in shows a blue shift of more than 40 nm, with respect to that of F8TBT-out. The photoluminescence (PL) spectra of F8TBT-in and F8TBT-out in solution overlap nearly completely with peak emission at around 640 nm, while in films it emerges at 636 nm for F8TBT-in and 655 nm for F8TBT-out. Hence, the PL spectrum of F8TBT-in shows a blue shift of 19 nm with respect to the analogue with alkyl side chains outwards (F8TBT-out). PLQE measurements are performed at two excitation wavelengths, 488 and 515 nm, to match the absorption peaks of F8TBT-in (≈470 nm) and F8TBT-out (≈500 nm), with films spin-coated onto quartz substrates with a thickness of ≈100 nm. As expected, it was found that the two different excitation wavelengths have no influence on the PLQE of F8TBT-in or F8TBT-out. The results (Table 1) show that the PLQE of F8TBT-in of 42% is almost four times larger than the PLQE of F8TBT-out (≈11%). The PLQE of F8TBT-in in solution was also measured, to determine the most suitable solvent for the best emissive performance, and the results indicate that p-xylene is the most appropriate choice (see Table S1, Supporting Information).

Table 1. The PLQE data of thin films of F8TBT-out and F8TBT-in with molecular weights of 50k g mol^{-1} (M_w).

Polymer	λ excitation = 488 nm	λ excitation = 515 nm
F8TBT-out	10.9%	10.6%
F8TBT-in	41.1%	40.5%

The time-correlated single photon counting (TCSPC) technique is adopted for the study of the fluorescence decay lifetime of both F8TBT-in and F8TBT-out films with thicknesses in the range of 30 nm. The excitation wavelength is at 470 nm and the decay rates are measured in the whole emission range, from 500 to 800 nm for F8TBT-in and from 580 to 780 nm for F8TBT-out, in steps of 20 nm. The TCSPC kinetics could not be fitted with single exponential decay curves, as they clearly showed a very fast and a slow decay component. The decay kinetics at each emission wavelength were therefore fitted with bi-exponential decay curves. The obtained fitting parameters, two lifetimes and two amplitudes at each wavelength, are shown in Figure 3a–c. The derived long lifetimes are in the range of 2.2 to 3.1 ns and 0.8 ns to 1.6 ns for F8TBT-in and F8TBT-out, respectively, while the short lifetime is less than 0.4 ns for both polymers, as shown in Figure 3a. Figure 4a and b show the emission spectra, integrated over time, obtained from the TCSPC measurements. The amplitudes of the short- and long-lived components,

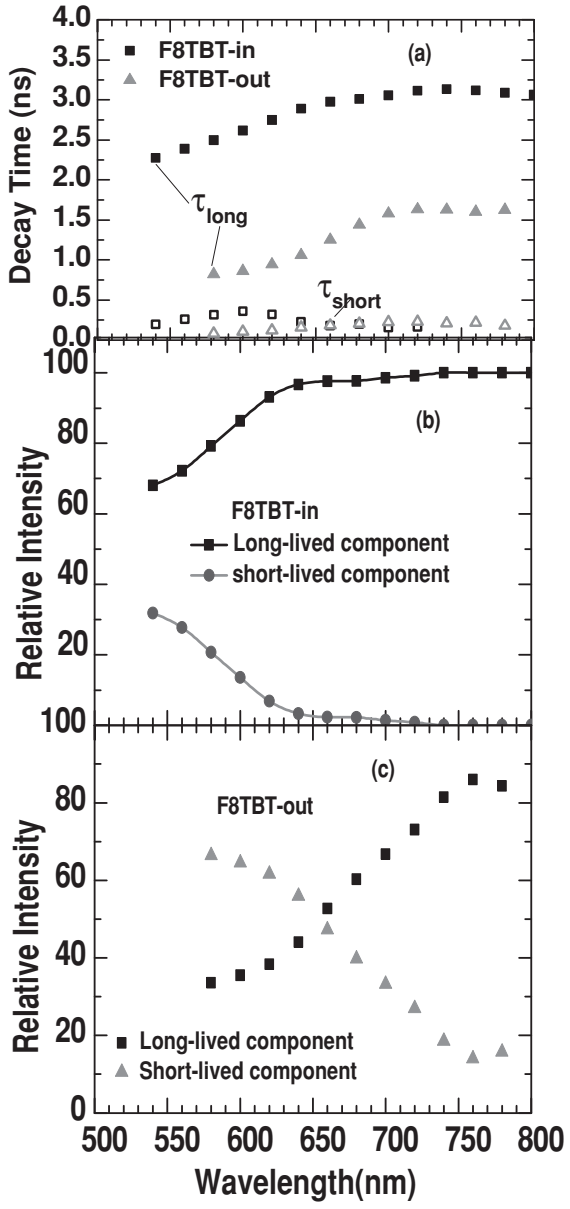

Figure 3. a) The decay lifetime of long-lived and short-lived components for F8TBT-in and F8TBT-out. b,c) The relative intensity of long-lived and short-lived components for: F8TBT-in (b) and F8TBT-out (c).

as obtained by the biexponential fit, are shown by the dashed and dotted lines, respectively. For F8TBT-in, the fast decay component is very weak and contributes little to the emission spectrum. However, for F8TBT-out the short-lived and long-lived components have very similar intensities, with the short-lived component prevailing at the high-energy side of the emission spectrum. Because of this blue-shift and the very fast decay, close to the instrumental resolution of our setup, we interpret the fast component to the phenomenon of exciton migration to lower energy sites within the polymer. The exciton migration

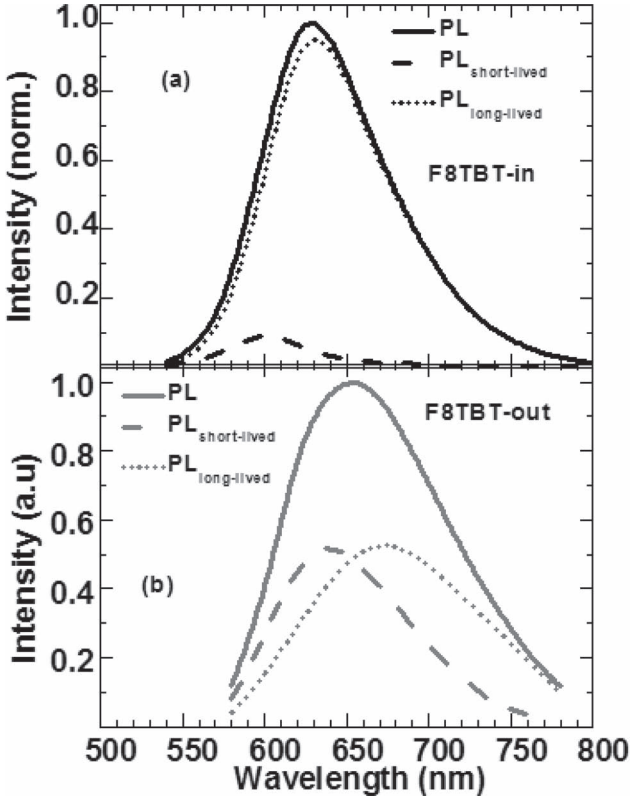

Figure 4. Time-integrated PL spectrum (solid line), together with the absolute PL spectra of the short-lived (dashed line) and long-lived (dotted line) components of: a) F8TBT-in and b) F8TBT-out.

from high-energy sites, caused by disorder such as kinks in the polymer backbone, to more ordered sites is therefore not necessarily a decay to the ground state, but can feed into the population of the longer-lived excitons. For this reason, we only use the slower decay component for the calculation of the radiative and non-radiative decay rates.

TCSPC measurements were also performed on both F8TBT polymers in solution. For F8TBT-in the decay time was very similar to that in film and the fast decay component was negligible. However, the decay time of F8TBT-out in solution was significantly increased to 4.2 ns and only a very weak fast decay component was observed (see Figure S1, Supporting Information). This further corroborates our assignment of the fast decay component to exciton diffusion.

Based on the results of PLQE and fluorescence lifetime, the radiative and non-radiative constants of F8TBT in film are calculated using the following equation:

$$\eta = \frac{k_r}{k_r + k_{nr}} = k_r \tau \quad (1)$$

where η is PLQE, k_r and k_{nr} are radiative and non-radiative constants, respectively, and τ is the measured fluorescence

Table 2. Summary of the radiative- and non-radiative decay constants of F8TBT-in and F8TBT-out.

	k_r [s^{-1}]	k_{nr} [s^{-1}]
F8TBT-out (50k g mol^{-1})	7.5×10^7	6.9×10^8
F8TBT-in (50k g mol^{-1})	1.4×10^8	2.1×10^8

lifetime. The decay lifetimes at the peak emission wavelength are 3 ns for F8TBT-in and 1.3 ns for F8TBT-out, corresponding to the long-lived component. The relevant results are summarized in Table 2, revealing that F8TBT-in shows a radiative constant almost two times larger than that of F8TBT-out, while the non-radiative constant of F8TBT-in is three times smaller. It is obvious that the variation of the side-chain position with respect to the benzothiadiazole (BT) unit induces the different optical properties between F8TBT-in and F8TBT-out; a study of the structural differences of these two polymers, by computational simulation, was thus carried out and is described in the next section.

2.2. Molecular Structure Simulation of F8TBT-out and F8TBT-in

The interchain interaction within conjugated polymers can be controlled by the introduction of side chains of a certain length and position. As the alkyl side chains in F8TBT-in are closer to each other, this could prevent a close packing of polymer chains and thus reduce the emission quenching. A computational simulation of the position of alkyl side chains with respect to the TBT units is carried out, and the geometries of F8TBT-out and F8TBT-in were optimized at the B3LYP/6-31G level using the GAMESS-UK package.[19] Hessian calculations showed that the optimized geometries are genuine minima (no imaginary frequencies). The resultant optimized geometries are depicted in Figure 5. It is clear that there is an obvious geometrical difference between F8TBT-in and F8TBT-out; it is likely that the alkyl side chains of F8TBT-in introduce a distortion within the TBT unit and the BT unit is no longer coplanar with the two thiophene rings. Hence, the alkyl side chains of F8TBT-in introduce distortion between the T-B-T units with dihedral angles of S-C-C-C being 128.4° and –130.1°, whereas these are 7.6° and 6.6° in the case of F8TBT-out. Hence the BT unit is no longer coplanar with the two thiophene rings in F8TBT-in while it is nearly coplanar for F8TBT-out. An efficient π–π overlap on the backbone of the polymer chain of F8TBT-in is therefore interrupted and the conjugation length shortened. This has an effect on the bandgap; for F8TBT-in, a bandgap of 2.81 eV is found, whereas for F8TBT-out, the calculated bandgap is 2.41 eV. This larger bandgap leads to a blue shift in both absorption and emission spectra of F8TBT-in, in agreement with the experimental data shown in Figure 2. A similar approach has been adopted to tune optoelectronic properties in low-bandgap donor–acceptor polymer systems, where this torsion in the backbone reduces the oscillator strength for the optical intrachain push–pull transition.[18] Furthermore, the high PLQE and decay constants of F8TBT-in are likely to be consequences arising from this structural distortion and will be discussed later.

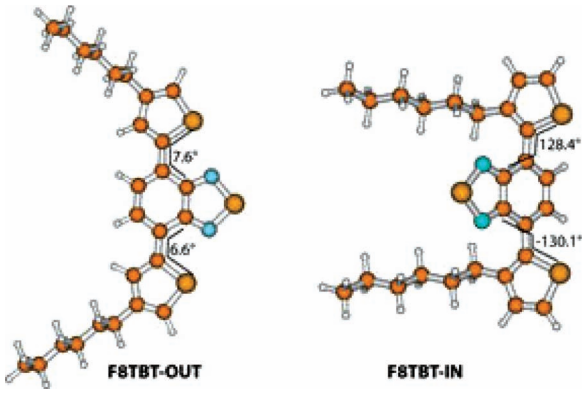

Figure 5. B3LYP/6-31G optimized geometries of the TBT section in F8TBT-out (left) and F8TBT-in (right). Dihedral S-C-C-C angles are as indicated; there is a distortion between the thiophene and benzothiadiazole units in F8TBT-in, which are nearly planar in the case of F8TBT-out.

2.3. LED Characteristics

To investigate the device performance of F8TBT-in and F8TBT-out, bipolar devices are fabricated in conventional (ITO/PEDOT:PSS/F8TBT-in or F8TBT-out/Ca/Al) and hybrid (ITO/ZnO/Cs_2CO_3/F8TBT-in or F8TBT-out/MoO_3/Au) structures; the experimental details have been described before.[20,21] Figure S2 in the Supporting Information gives the schematic energy level diagram in both the HyLEDs and conventional LEDs, and device structures. The HOMO and LUMO levels of F8TBT-out are 5.6 and 3.5 eV; and 5.5 eV and 3.3 eV for F8TBT-in, which are thus slightly shifted with respect to its parent analogue (the HOMO level was measured by cyclic voltammetry and the UV–vis absorption spectra bandgap was added to estimate the LUMO level). However, the theoretical calculations for the optimized geometries show different values for the HOMO and LUMO levels; 5.32 and 2.91 eV, respectively for F8TBT-out, and 5.73 and 2.92 eV for F8TBT-in. The calculated HOMO and LUMO levels are thus somewhat different from the measured ones. However, the bandgap derived from the calculation is 2.81 eV for F8TBT-in and 2.41eV for F8TBT-out, which seems consistent given the large blue-shift observed in the absorption spectra (see Figure 2). The emissive layer in devices is ≈100 nm thick and is annealed at 120 °C for 1 h after spin-coating onto the Cs_2CO_3 interlayer.

Electroluminescence studies of F8TBT-in and F8TBT-out were performed on the HyLED structures, as shown in Figure 6. The EL spectra are similar, with a slight blue-shift

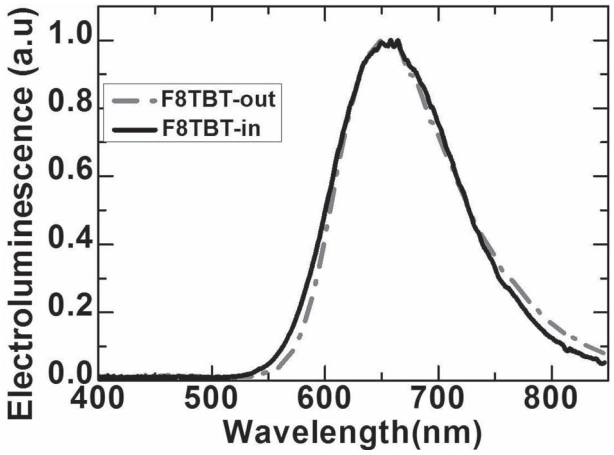

Figure 6. Electroluminescence (EL) spectra of F8TBT-out and F8TBT-in, for thin polymer films, which have been annealed at 120 °C. The EL emission peaks are nearly overlapped.

for F8TBT-in with respect to F8TBT-out; the emission peak of F8TBT-in is at 664 nm and that of F8TBT-out at 658 nm. In contrast to some reports in the literature,[16] where the EL peaks are generally blue-shifted by 10 nm with respect to the PL, the EL peak (664 nm) of F8TBT-in is significantly red-shifted with respect to its PL peak (636 nm). Interestingly, there is no significant difference between the PL and EL spectral peaks in the case of F8TBT-out, which are 658 nm for EL and 655 nm for PL, as summarized in Table 3. More remarkably, when the emissive layer is not annealed (in a conventional structure), the EL spectra of F8TBT-in shows a blue-shift (19 nm) with respect to that of F8TBT-out (not shown). However, the EL spectrum of annealed F8TBT-out shows little red-shift in emission peaks with respect to the PL and EL of its unannealed analogue (see Table 3). This observation is consistent with changes in the geometry of TBT units upon annealing, which is also in good agreement with the results from the PL spectra in solution where the PL spectra of F8TBT-in and F8TBT-out are overlapped as the inter-molecular interaction are significantly reduced in solution for F8TBT-out. However, there is little such influence in the case of F8TBT-in, due to the geometric distortion on the backbone caused by the side-chain positions.

Figure 7 shows the *J–V–L* characteristics and derived current efficiency using F8TBT-in and F8TBT-out as the

Table 3. Summary of peak emission wavelengths in photoluminescence (PL) and electroluminescence (EL) of F8TBT-in and F8TBT-out. Samples were annealed or unannealed as indicated.

	$\lambda_{PL\ Max.}$ (unannealed) [nm]	$\lambda_{EL\ Max.}$ (unannealed) [nm]	$\lambda_{EL\ Max.}$ (annealed) [nm]
F8TBT-in	636	642	664
F8TBT-out	655	661	658

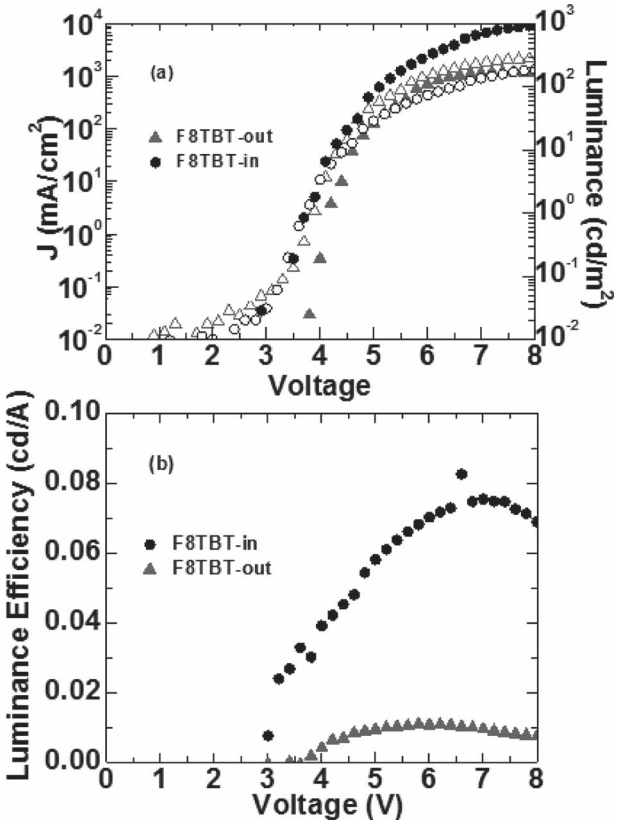

Figure 7. a) The *J–V–L* curves of F8TBT-in and F8TBT-out in a conventional PLED structure; the open symbols represent current density and solid symbols luminance, gray triangles for F8TBT-out and black circles for F8TBT-in. b) Luminance efficiency for F8TBT-out (gray) and F8TBT-in (black), as derived from (a).

emissive layer in a conventional LED structure. The current density of F8TBT-out is slightly higher than that of F8TBT-in, but the magnitude of brightness of F8TBT-in is much greater. Also, the luminance turn-on of F8TBT-in is lower than that of F8TBT-out, as shown in Figure 7a. The derived current efficiency is plotted in Figure 7b, as a consequence of higher luminance and lower current density, F8TBT-in shows a eight times higher luminance efficiency. The parameters obtained from Figure 7 are summarized in Table 4. The devices with hybrid structure were not as stable as conventional devices; due to unintentional doping by Cs_2CO_3 and MoO_3 interlayers, as the emissive layer was thin (100 nm).[20] However, these devices also showed a much greater efficiency in the case of F8TBT-in

Table 4. Summary of conventional LED device characteristics.

	Current efficiency [cd A^{-1}]	Maximal luminance [cd m^{-2}]	Luminance turn-on [V]
F8TBT-in	0.084	960	2.9
F8TBT-out	0.015	174	3.8

as the emissive layer compared with that of F8TBT-out and the results are summarized in the Supporting Information (see Supporting Information, Table S2).

3. Discussion

The optical study of these two polymers suggests that the higher PLQE of F8TBT is attributed to a higher radiative decay constant and reduced non-radiative constant. The PL spectra of F8TBT-in and F8TBT-out in solution are nearly overlapped with each other, while the peak luminance of F8TBT-out shows a 19 nm redshift with respect to that of F8TBT-in in the case of film. Note that the films for PL performance are not annealed in contrast with the EL spectra of F8TBT-in and F8TBT-out recorded from HyLEDs, which are almost completely overlapped upon annealing at 120 °C. In the case of F8TBT-out, the annealing treatment has very little influence on the emission peak; hence the PL and EL spectra have very little shift relative to each other upon annealing (see Table 3). The computational simulation of the alkyl side-chain geometries with respect to TBT units (see Figure 5) suggests a plausible explanation for this observation. The BT unit in F8TBT-in is not coplanar with the two thiophene rings, in contrast to the coplanar geometry of F8TBT-out.[18] However, the conformation changes upon annealing, with the BT unit of F8TBT-in becoming coplanar,[22] as the heating treatment supplies the necessary activation energy. This coplanar conformation of TBT units indeed increases the π–π conjugation length of the backbone and leads to a red-shift of the EL spectrum upon annealing. Therefore the EL spectrum of F8TBT-in is very similar to that of the F8TBT-out upon annealing. For the same reason, the annealing treatment has very little influence on the EL spectra of F8TBT-out as the TBT units are already coplanar. However, the side-chain effect still makes a difference on the degree of close packing of the two kinds of polymers. The two alkyl side chains in F8TBT-in are closer to each other, leading to a larger steric hindrance, which is likely to prevent the close packing of interchains and reduce exciton quenching. The blue-shift in the PL as well as EL of F8TBT-in is an indication of the interrupted π-π conjugation and reduced interchain interaction, and the latter is also reflected in the device performance in both conventional and hybrid structures. The devices using F8TBT-in show a 17 times higher luminous efficiency than the device with F8TBT-out in the hybrid structure as summarized in Table 4 and S2 in the Supporting Information.

While the device performance in conventional and hybrid structures is generally comparable, we note that some aspects of these results and discussion are not entirely conclusive. Previous studies demonstrate that the hybrid structure with Cs_2CO_3 shows better device performance with a thicker film (more than 100 nm), as the effect of Cs_2CO_3 diffusion leading to defects at the interface of Cs_2CO_3/polymer is less pronounced in a thick film.[20,23]

Unfortunately, a study of device performance with thicker films of F8TBT-in and F8TBT-out is absent in the present study, due to the lack of further supply of the polymers. However, a thickness dependence study based on the F8TBT-out with a molecular weight of 423 k manufactured by CDT showed a similar trend; the thicker the better, with remarkably high luminance. These results are presented in Table S3 in the Supporting Information. The optical studies reveal that both the PLQE and decay constants of F8TBT-out from CDT are similar to those of F8TBT-in with a low molecular weight of 50k g mol^{-1} (see Table S4 and S5, Supporting Information). The PLQE of F8TBT-out increases with the increase of the molecular weight (Table S4, Supporting Information). These variations due to molecular weight have been observed in the case of other green emitting PFOs,[22] and may also have been related to purity issues. This implicates that F8TBT-in with a higher molecular weight might have a scope for further synthetic improvement. The lab scale of synthesis is not comparable with the industrial level in the terms of purity and molecular weight; this might explain why the device performance of F8TBT-in and F8TBT-out reported here is rather poor. Nevertheless, the F8TBT-in and F8TBT-out synthesized in the same laboratory should have similar random and systematic errors, and are therefore comparable.

In general, these results offer a strong demonstration that F8TBT-in is more promising in LED applications than F8TBT-out. Furthermore, the concept of using molecular design in order to tune the optical and electrical properties, based on theoretical predictions, is highlighted by the experiment results. Also, an improved quality of the F8TBT-in material, with higher molecular weight and purity should offer an optimal performance.

4. Conclusion

The effect of the positioning of alkyl side-chains on the thiophene rings of F8TBT has been studied in terms of optical properties and devices performance. The optical measurements show that the absorption of F8TBT-in within a thin film (100 nm) has a 47 nm blue-shift compared with that of its parent analogue F8TBT-out; the PL spectrum of F8TBT-in demonstrates a blue shift of 19 nm compared with that of F8TBT-out, this consequently leads to reduced spectral overlap between the absorption and PL, hence resulting in reduced self-absorption in the case of polymer F8TBT-in. Fluorescence decay measurements show a longer lifetime for F8TBT-in, as compared with that of F8TBT-out. A computational simulation reveals that the BT units are distorted out of the coplanar arrangement

formed by the thiophene rings, and this leads to an interrupted π–π conjugation and consequently a larger bandgap between HOMO and LUMO. The study of device performance using F8TBT-in and F8TBT-out has demonstrated that the current efficiency and luminance efficiency of F8TBT-in is much improved. This is in good agreement with the expectation that a larger steric hindrance caused by the side chains can prevent close packing, reducing the exciton quenching. Further investigation on different molecular weight indicates that F8TBT with higher molecular weight gives increased PLQE, as well as improved device performance. On a more general level, these experimental studies highlight the concept of using molecular design in order to tailor the optical and electrical properties, based on theoretical predictions.

Supporting Information

Supporting Information is available from the Wiley Online Library or from the author.

Acknowledgements: This work was supported by Cambridge Display Technology (CDT Ltd) and Cambridge European Trust. R.W.A.H. acknowledges the Zernike Institute for Advanced Materials for financial support ("Dieptestrategie" program). C.E.F. thanks the Royal Society (UK) for a Research Grant.

Received: November 23, 2012; Revised: February 7, 2013; Published online: March 13, 2013; DOI: 10.1002/macp.201200681

Keywords: conjugated polymers; light-emitting diodes (LEDs); organic electronics

[1] M. Gross, D. C. Müller, H.-G. Nothofer, U. Scherf, D. Neher, C. Bräuchle, K. Meerholz, *Nature* **2000**, *405*, 661.
[2] a) M. A. Stevens, *High-Intensity Optical Excitation of Conjugated Polymers*, Ph.D. Thesis, University of Cambridge, **2000**; b) N. K. Patel, S. Cina, J. H. Burroughes, *IEEE J. Sel. Top. Quantum Electron.* **2002**, *8*, 346.
[3] Q. Hou, Y. Xu, W. Yang, M. Yuan, J. Peng, Y. Cao, *J. Mater. Chem.* **2002**, *12*, 2887.
[4] M. Inbasekaran, E. P. Woo, W. S. Wu, M. T. Bernius, *PCT application*, *W0046321A1*, **2000**.
[5] R. Xia, G. Heliotis, Y. Hou, D. D. C. Bradley, *Org. Electron.* **2003**, *4*, 165.
[6] E. P. Woo, M. Inbasekaran, W. Shiang, G. R. Roof, *WO 9905184*, **1997**.
[7] O. Inganäs, M. Svensson, F. Zhang, A. Gadsia, N. K. Persson, X. Wang, M. R. Andersson, *Appl. Phys. A: Mater. Sci. Process.* **2004**, *79*, 31.
[8] C. Shi, Y. Yao, Y. Yang, Q. Pei, *J. Am. Chem. Soc.* **2006**, *128*, 8980.
[9] P. Wang, A. Abrusci, H. M. P. Wong, M. Svensson, M. R. Andersson, N. C. Greenham, *Nano Lett.* **2006**, *6*, 1789.
[10] C. R. McNeill, A. Abrusci, J. Zaumseil, R. Wilson, M. J. McKiernan, J. H. Burroughes, J. J. M. Halls, N. C. Greenham, R. H. Friend, *Appl. Phys. Lett.* **2007**, *90*, 193506.
[11] C. R. McNeill, J. J. M. Halls, R. Wilson, G. L. Whiting, S. Berkebile, M. G. Ramsey, R. H. Friend, N. C. Greenham, *Adv. Funct. Mater.* **2008**, *18*, 1.
[12] J. Zaumseil, C. R. McNeill, M. Bird, D. L. Smith, P. P. Ruden, M. Roberts, M. J. McKiernan, R. H. Friend, H. Sirringhaus, *Appl. Phys. Lett.* **2007**, *90*, 193506.
[13] H. J. Bolink, H. Brine, E. Coronado, M. Sessolo, *ACS Appl. Mater. Interfaces* **2010**, *2*, 2694.
[14] N. Drolet, S. Beaupre, J.-F Morin, Y. Tao, M. J. Leclerc, *Opt. A: Pure Appl. Opt.* **2002**, *4*, S252.
[15] I. S. Millard, *Synth. Met.* **2000**, *111*, 119.
[16] Q. Hou, Q. Zhou, Y. Zhang, W. Yang, R. Yang, Y. Cao, *Macromolecules* **2004**, *37*, 6299.
[17] G. Tu, S. Massip, P. M. Oberhumer, X He, R. H. Friend, N. C. Greenham, W. T. S. Huck, *J. Mater. Chem.* **2010**, *20*, 9231.
[18] P. M. Oberhumer, Y.-S. Huang, S. Massip, D. T. James, G. Tu, S. Albert-Seifried, D. Beljonne, J. Cornil, J.-S. Kim, W. T. S. Huck, N. C. Greenham, J. M. Hodgkiss, R. H. Friend, *J. Chem. Phys.* **2011**, *134*, 114901.
[19] M. F. Guest, I. J. Bush, H. J. J. van Dam, P. Sherwood, J. M. H. Thomas, J. H. van Lenthe, R. W. A. Havenith, J. Kendrick, *Mol. Phys.* **2005**, *103*, 719.
[20] a) D. Kabra, L. P. Lu, M. H. Song, H. J. Snaith, R. H. Friend, *Adv. Mater.* **2010**, *22*, 3194; b) D. Kabra, M. H. Song, B. Wenger, R. H. Friend, H. J. Snaith, *Adv. Mater.* **2008**, *18*, 3447; c) M. H. Song, D. Kabra, B. Wenger, R. H. Friend, H. J. Snaith, *Adv. Funct. Mater.* **2009**, *19*, 2130.
[21] L. P. Lu, D. Kabra, K. Johnson, R. H. Friend, *Adv. Funct. Mater.* **2012**, *11*, 144.
[22] C. L. Donley, J. Zaumseil, J. W. Andreasen, M. M. Nielsen, H. Sirringhaus, R. H. Friend, J.-S. Kim, *J. Am. Chem. Soc.* **2005**, *127*, 12891.
[23] L. P. Lu, D. Kabra, R. H. Friend, *Adv. Funct. Mater.* **2012**, *22*, 4165.